

Interplay of electronic and nuclear degrees of freedom in a femtosecond-scale photochemical reaction

Yusheng Dou^a Ben R. Torralva^b Roland E. Allen^a

^a*Institute for Quantum Studies and Department of Physics,
Texas A&M University, College Station, TX 77843*

^b*Chemistry and Materials Science,
Lawrence Livermore National Laboratory, Livermore, CA 94550*

Abstract

The intricate dynamical processes in photochemical reactions are not fully accessible to either experiment or conventional theory. Here we outline a technique for realistic simulations in photochemistry, and demonstrate that it provides a remarkably successful description of photoisomerization. One observes a nontrivial sequence of events which include multiple electronic excitations, conversion of double bonds to single bonds (and vice-versa), nonadiabatic depopulation of excited levels at avoided crossings, vibrational energy redistribution, and an elegant interdependence of the various electronic and vibrational degrees of freedom.

Femtosecond-scale processes are enormously important in physics, chemistry [1], and biology [2]. Examples are the molecular processes which lead to bond breaking and formation [3], photoisomerization of retinal as the primary event in vision [4,5], energy transfer in photosynthesis [6], and the dynamics of electronically excited states in DNA [7,8]. Major achievements in this general area include the discovery that the 11-cis to all-trans torsional isomerization of retinal in rhodopsin is essentially completed in only 200 fs [9,10] and recent successes related to quantum control of chemical reactions [11–13].

Despite the impressive progress of recent years, many detailed features of femtosecond-scale processes are still not accessible to either experiments or standard theories, because the time scales are short, the intensities of the experimental laser pulses are high, and the most interesting molecules have many degrees of freedom. There is thus an important role for realistic simulations, which reveal more detail than the experiments, but do not require the approximations of standard theory.

Here we outline a relatively new technique for realistic simulations of femtosecond-scale molecular processes, and demonstrate its power for providing insight into the detailed dynamics. Although there are many approaches in the chemistry and physics literature for simulating such processes [14–16], we are not aware of any other work which has addressed the complete sequence of events that begins with the application of a laser pulse to a molecule. There is not sufficient space here to do justice to the large volume of previous theoretical studies, but we mention that much of this work has involved calculations of potential energy surfaces, molecular dynamics simulations of atomic motion, etc., rather than full simulations of the dynamics of electrons and nuclei coupled to an applied laser radiation field.

One common procedure is simply to promote electrons to an excited-state energy surface. This approach can provide useful information regarding molecular evolution, but it is completely incapable of treating the influence of laser pulse parameters on the outcome, an aspect of critical importance in the emerging area of quantum control [11,13]. With the present method, one can vary the laser pulse shape, duration, intensity, polarization, and phase, and study how these features affect the relative yield of different products. In addition, one can monitor the electronic and nuclear dynamics in complete detail, to obtain an understanding of the interplay between the various degrees of freedom.

The method employed here is an extension of that used earlier for other systems [18,19,17] and has two particularly important features: First, it has proved to give a reliable description of bonding [17], largely because the parameters which determine the Hamiltonian and ion-core repulsion are determined in density-functional calculations [20]. Second, it is quite straightforward: One sets up the molecule with initial conditions, applies a laser pulse with the desired characteristics, and then observes the response of electrons and nuclei as a function of time. There is no need to force the “hopping” of electrons from one energy surface to another, or to intervene in any other way. As will be seen below, nonadiabatic processes are found to occur automatically. The present method, like any semiclassical approach, effectively includes the absorption and stimulated emission of photons and vibrational quanta.

The electron dynamics is treated by solving the time-dependent Schrödinger equation in a nonorthogonal basis, using a unitary algorithm which is based on iterative solution of the equation for the time evolution operator:

$$\Psi_j(t + \Delta t) = \mathbf{U}(t + \Delta t, t) \cdot \Psi_j(t) \quad (1)$$

$$\mathbf{U}(t + \Delta t, t) = (\mathbf{1} + (i/2\hbar) \Delta \mathbf{I})^{-1} (\mathbf{1} - (i/2\hbar) \Delta \mathbf{I}) \quad (2)$$

$$\Delta \mathbf{I} = \int_t^{t+\Delta t} dt' \mathbf{H}(t') \quad (3)$$

with $\Psi_j = \mathbf{S}^{1/2}\bar{\Psi}_j$ and $\mathbf{H} = \mathbf{S}^{-1/2}\bar{\mathbf{H}}\mathbf{S}^{-1/2}$. Here $\bar{\mathbf{H}}$, \mathbf{S} , and $\bar{\Psi}_j$ are the original Hamiltonian matrix, overlap matrix, and state vector for electron j in the nonorthogonal basis. The motion of the atomic nuclei is determined from a generalized Ehrenfest theorem:

$$M\ddot{X} = -\sum_j \Psi_j^\dagger \cdot (\partial\mathbf{H}/\partial X) \cdot \Psi_j - \partial U_{rep}/\partial X \quad (4)$$

where M and X are any nuclear mass and coordinate. The electrons are coupled to the vector potential \mathbf{A} of the radiation field through the time-dependent Peierls substitution

$$H_{ab}(\mathbf{X} - \mathbf{X}') = H_{ab}^0(\mathbf{X} - \mathbf{X}') \exp(iq\mathbf{A} \cdot (\mathbf{X} - \mathbf{X}')/\hbar c) \quad (5)$$

where a labels an orbital and \mathbf{X} a nuclear position.

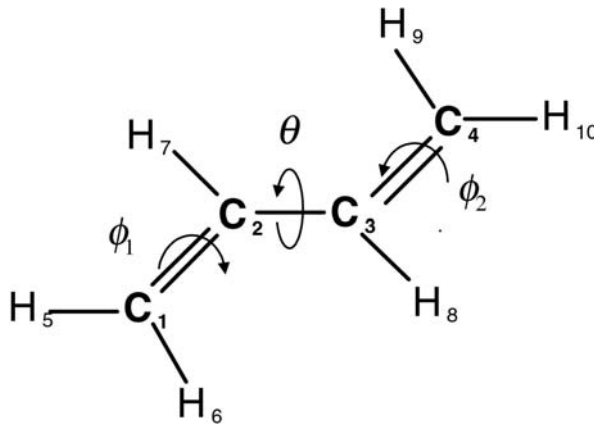


Fig. 1. Structure of trans-butadiene, with definitions of the internal coordinates.

As an example of the capabilities of this method, we now present results for a representative reaction which exhibits some rather subtle features: namely, photoisomerization of trans-butadiene, whose structure is shown in Fig. 1. Before a laser pulse is applied, the molecule is allowed to relax, and its equilibrium geometry is found to be in close agreement with experiment [21]. To be more specific, let us consider the three torsional angles θ , ϕ_1 , and ϕ_2 , respectively defined by C₁-C₂-C₃-C₄, H₅-C₁-C₂-C₃, and C₂-C₃-C₄-H₉. Rotation around the central C-C bond is described by θ , and rotation around the two terminal bonds by ϕ_1 and ϕ_2 . In the equilibrium geometry, the values of these angles were found to be $\theta = 180^\circ$, $\phi_1 = -180^\circ$, and $\phi_2 = 0^\circ$.

A laser pulse with a Gaussian profile was then applied, with the following parameters: full-width-at-half-maximum (FWHM) duration of 75 fs, photon energy centered at 4.2 eV, and fluence of 0.90 kJ/m². The photon energy was chosen to approximately match the density-functional energy gap between the HOMO and LUMO. This value of the fluence was chosen because it was found to produce a conformational change without bond-breaking. Fuss and coworkers [22] employed a similar laser pulse in their pump-probe experiments.

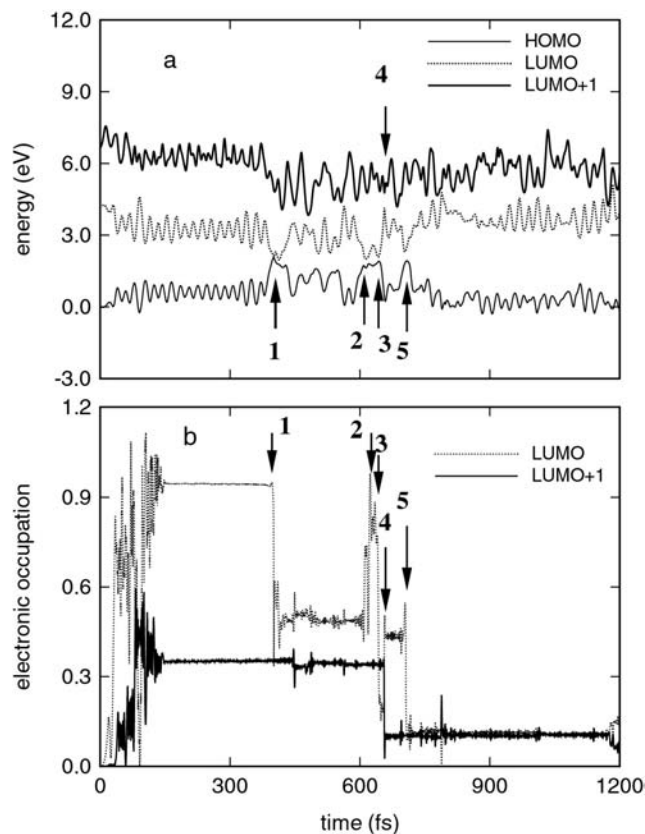


Fig. 2. (a) Variation of HOMO, LUMO and LUMO+1 orbital energies with time. The five avoided crossings are labeled 1,2, ..., 5. (b) Electron occupancy of LUMO and LUMO+1 orbitals. Rapid electronic transitions are observed at each avoided crossing.

In Fig. 2, energies are shown as functions of time for the (initially) highest occupied molecular orbital (HOMO) and lowest unoccupied molecular orbital (LUMO), as well as the LUMO+1. The time-dependent populations of these orbitals are also shown. Figure 3 shows the same quantities on an expanded scale during the period that the laser pulse is applied (the first 150 femtoseconds, since the FWHM duration is 75 fs). During this period about 0.95 electrons are promoted from the HOMO to the LUMO, and 0.35 to the LUMO+1. It is interesting that occupancy of the LUMO+1 primarily results from excitation out of the LUMO, at a time when the separation of these two excited states momentarily matches the photon energy of 4.2 eV. This symmetry-allowed transition occurs at about 85 fs.

In the crudest picture, there are two stages in photoisomerization: First, excitation of electrons temporarily modifies the bonding, permitting the molecule to undergo a conformational change. Second, the excited electrons undergo nonradiative downward transitions, so that the molecule is eventually locked in the electronic ground state with a new geometry. Since the vibrational quanta have relatively low energies, these nonradiative transitions have a high

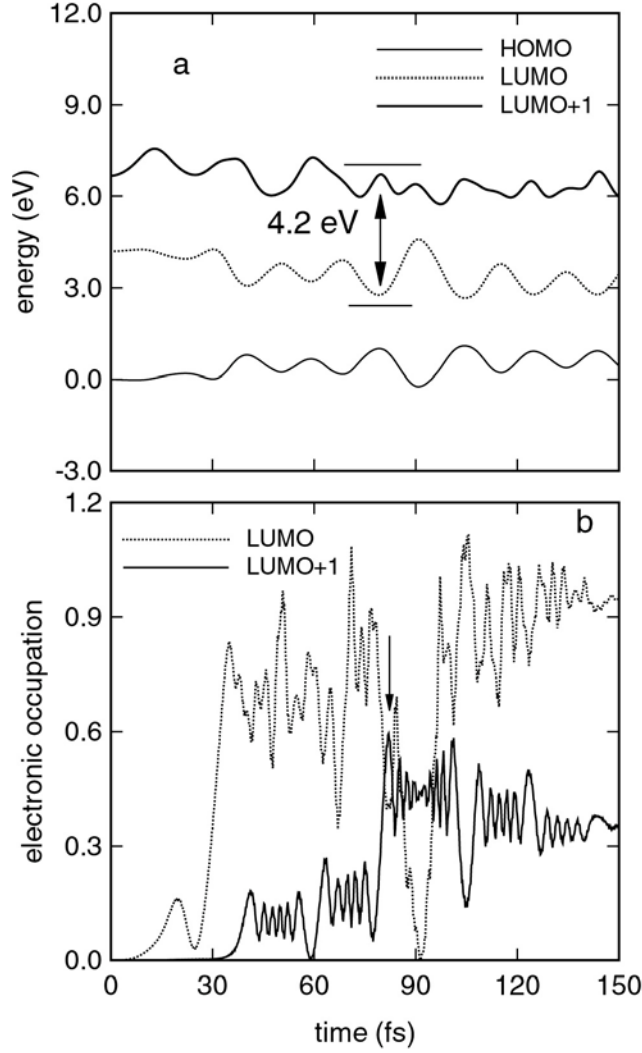


Fig. 3. Same quantities as in Fig. 3, but with an expanded scale to emphasize important features during the first 150 femtoseconds.

probability only when the electronic levels exhibit close approaches, at avoided crossings.

Five such avoided crossings can be seen in Fig. 2, at 402, 618, 643, 656, and 705 fs, and each of these events is associated with rapid electronic transitions. The energy gaps are respectively found to be 0.01, 0.29, 0.17, 0.65, and 0.45 eV. Notice that nonadiabatic couplings 1, 3, and 5 induce LUMO \rightarrow HOMO transitions; 4 induces a LUMO+1 \rightarrow LUMO transition; and 2 induces HOMO \rightarrow LUMO. Between 705 and 800 fs, the HOMO-LUMO gap increases to about 4.0 eV, and then remains at this value, but by this time the excited states have been effectively depopulated.

All these avoided crossings occur in conjunction with ϕ_1 and ϕ_2 rotations between about 400 and 710 fs, which can be seen in Fig. 4. The variations in

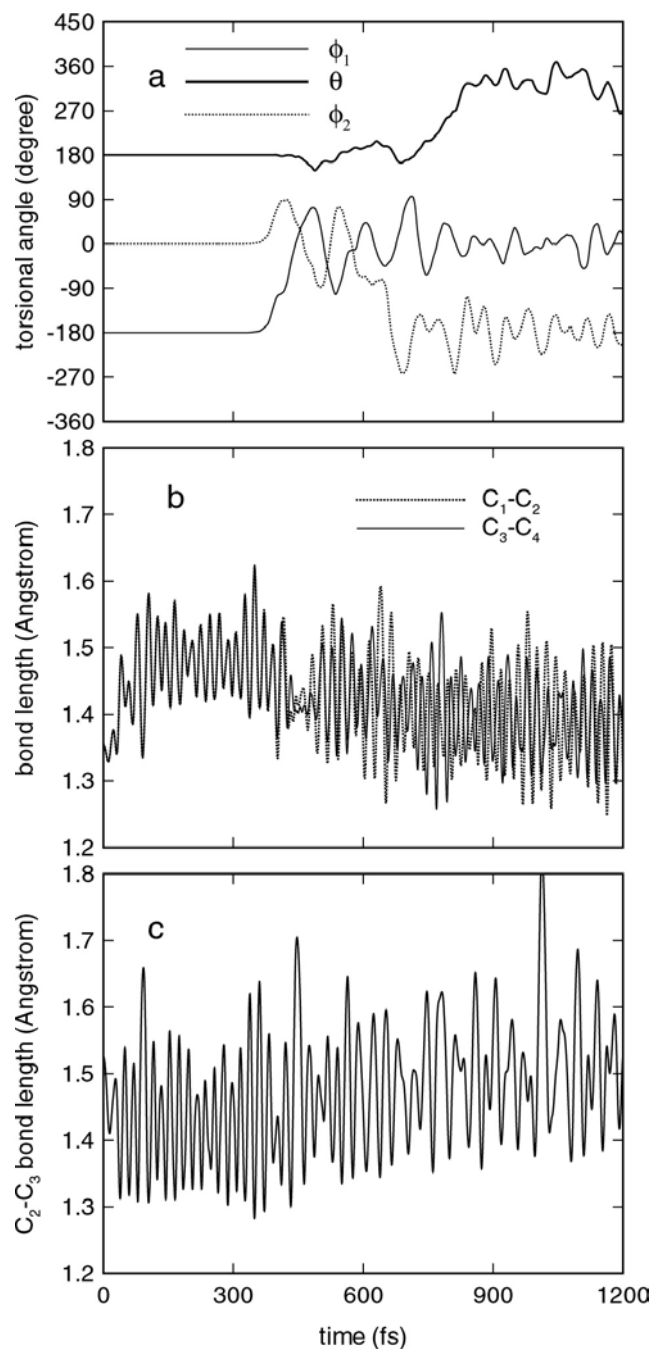


Fig. 4. (a) Change in torsional angles θ , ϕ_1 , and ϕ_2 . (b) Variation of C_1-C_2 and C_3-C_4 bond lengths with time. (c) Variation of C_2-C_3 bond length.

C-C bond lengths are also shown in this figure: Each terminal C-C bond is lengthened, from 1.35 to 1.48 Å, demonstrating that each has been effectively converted from a double to a single bond. The central C-C bond undergoes the opposite kind of change, from single to double bond, with its length temporarily shortened from 1.5 to 1.4 Å. At the same time, the C-C stretching frequency is found to temporarily decrease for the terminal bonds and increase for the central bond.

These changes are due to the anti- π -bonding character of the LUMO and LUMO+1 orbitals, and they play a major role in determining how the isomerization proceeds: As can be seen in Fig. 4 (a), the butadiene molecule twists about the two terminal C-C bonds after 400 fs, but rotation about the central bond is delayed until about 800 fs. In each case, rotation proceeds around a single bond, and not a more rigid double bond.

Figure 4 shows that the stretching modes of both central and terminal C-C bonds are excited when electrons are promoted to the LUMO level, because of the sudden change in the Hellmann-Feynman forces on the nuclei. A subsequent increase in vibrational amplitude for the terminal bonds, after 400 fs, is due to the release of electronic energy during nonadiabatic events.

Starting from the initial equilibrium geometry in the electronic ground state, θ , ϕ_1 , and ϕ_2 each rotate through approximately $\pm 180^\circ$ (with the rotations completed at about 800, 450 and 700 fs respectively). The molecular geometry subsequently remains fixed, except for torsional oscillations and other residual vibrations.

These results clearly reveal the elegant interdependence of electronic and nuclear degrees of freedom: During the first 150 fs, as the laser pulse is applied, electrons are promoted from HOMO to LUMO and LUMO to LUMO+1 via one-photon transitions. These electronic excitations alter the forces on the nuclei, exciting C-C stretch vibrations, and they also change the character of the C-C bonds: The central bond effectively becomes a double bond, with shorter bond length, higher vibrational frequencies, and more rotational rigidity. The two terminal bonds, on the other hand, effectively become single bonds, permitting the ϕ_1 and ϕ_2 rotations of Fig. 4, which are activated by vibrational energy redistribution from the modes initially excited.

These rotations alter the molecular orbitals and their energy levels, and are largely responsible for the series of avoided crossings in Fig. 2. At each of these points of closest approach, there is stimulated emission (or absorption) of vibrational quanta, with the electrons undergoing downward (or upward) transitions. The final result is a depopulation of the excited states, restoring the original character of the terminal and central C-C bonds. The θ rotation then becomes possible, and it is activated by the energy released from the electrons at avoided crossings. After less than a picosecond, the original “stretched-out” trans-butadiene has been converted to “folded-over” cis-butadiene, in which C_1 and C_4 have been brought closer together by a rotation of approximately 180° around the central bond.

The specific example treated here, photoisomerization of trans-butadiene, is a relatively simple photochemical reaction. It nevertheless demonstrates the power of realistic simulations to reveal underlying mechanisms in great detail.

The crucial features of the present method are that it incorporates the coupled dynamics of all relevant electronic and vibrational degrees of freedom, and that it treats the response to a laser pulse with arbitrary shape, duration, and intensity.

Acknowledgements

This work was supported by the Robert A. Welch Foundation, ONR, and DARPA. The work of B.R.T. was performed under the auspices of the U.S. Department of Energy and Lawrence Livermore National Laboratory, Contract No. W-7405-Eng-48.

References

- [1] A. H. Zewail, *Femtochemistry: Ultrafast Dynamics of the Chemical Bond* (World Scientific, Singapore, 1998).
- [2] R. S. Knox, *J. Photochem. Photobiol. B* **49**, 81 (1999).
- [3] A. H. Zewail, *Angew. Chem. Int. Ed.* **39**, 2587 (2000).
- [4] R. A. Mathies, *Novartis Foundation Symposium 224: Rhodopsins and Phototransduction* (Wiley, Chichester, 1999), p.70.
- [5] R. R. Birge, *Annu. Rev. Phys. Chem.* **41**, 683 (1990).
- [6] H. van Amerongen, L. Valkunas, and R. van Grondelle, *Photosynthetic Excitons* (World Scientific, Singapore, 2000).
- [7] C. Z. Wan, T. Fiebig, S. O. Kelley, C. R. Treadway, J. K. Barton, and A. H. Zewail, *Proc. Natl. Acad. Sci. USA* **96**, 6014 (1999).
- [8] J. M. L. Pecourt, J. Peon, and B. Kohler, *J. Am. Chem. Soc.* **122**, 9348 (2000).
- [9] R. W. Schoenlein, L. A. Peteanu, R. A. Mathies, and C. V. Shank, *Science* **254**, 412 (1991).
- [10] M. O. Trulson, and R. A. Mathies, *J. Phys. Chem.* **94**, 5741 (1990).
- [11] R.S. Judson and H. Rabitz, *Phys. Rev. Lett.* **68**, 1500 (1992).
- [12] R. J. Levis, G. M. Menkir, and H. Rabitz, *Science* **292**, 709 (2001).
- [13] H. Rabitz, *Science* **299**, 525 (2003), and references therein.
- [14] J. C. Tully, in *Classical and Quantum Dynamics in Condensed Phase Simulations*, edited by B. J. Berne, G. Ciccotti, and D. F. Coker (World Scientific, Singapore, 1998).

- [15] W. Domcke and G. Stock, *Adv. Chem. Phys.* **100**, 1 (1997).
- [16] M. Ben-Nun and T. J. Martínez, *Adv. Chem. Phys.* **121**, 439 (2002).
- [17] B. Torralva, T. A. Niehaus, M. Elstner, S. Suhai, Th. Frauenheim, and R. E. Allen, *Phys. Rev. B* **64**, 153105 (2001).
- [18] J. S. Graves and R. E. Allen, *Phys. Rev. B* **58**, 13627 (1998)
- [19] T. Dumitrica and R. E. Allen, *Phys. Rev. B* **66**, 081202 (2002).
- [20] M. Elstner, D. Porezag, G. Jungnickel, J. Elsner, M. Haugk, Th. Frauenheim, S. Suhai, and G. Seifert, *Phys. Rev. B* **58**, 7260 (1998) and references therein.
- [21] R. H. Baughman, B. E. Kohler, I. J. Levy and C. Spangler, *Synthetic Metals* **11**, 37 (1985).
- [22] W. Fuss, W. E. Schmid and S.A. Trushin, *Chem. Phys. Lett.* **342**, 91 (2001).